Cal X-1: an absolute in-orbit calibrator for current and future X-ray observatories

Project White Paper for Astro-2020 Decadal Survey

Type of activity: Space-Based Project

Authors: Keith Jahoda[1,5,*], Maxim Markevitch[1], Takashi Okajima[1], Joanne Hill-Kittle[1], Neerav Shah[1], Denis Bergeron[2], Andrew Holland[3], Paul Plucinsky[4,5], Dan Schwarz[4,5]

[1]NASA Goddard [2]NIST [3]Open University, UK [4]Harvard-Smithsonian CfA
[5]IACHEC [*]keith.jahoda@nasa.gov

Endorsed by: Belinda Wilkes (*Chandra* X-ray Center Director),
Norbert Schartel (*XMM-Newton* Project Scientist),
Matteo Guainazzi (*Athena* Study Scientist, *XRISM* ESA Project Scientist)

July 10, 2019

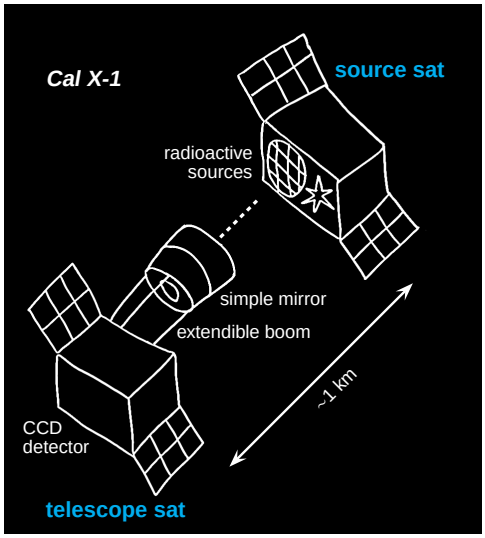

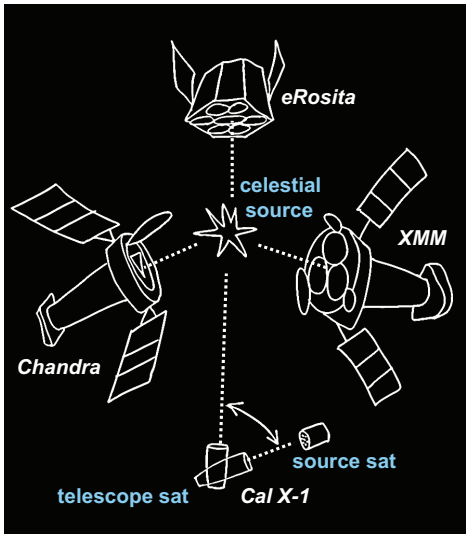

1 SUMMARY

X-ray astronomy is now making observations relevant to fundamental physics and cosmology. However, the constraining power of many of these measurements is limited by the instrument calibration uncertainty. Cross-comparison of the most powerful X-ray observatories in existence, which have also had the most systematic and thorough ground calibration programs ever, reveal systematic discrepancies in the measured source fluxes at a $> 10\%$ level. Clearly, ground calibration alone cannot provide a better accuracy because of its inherent limitations and the changes that the observatories experience on their way to orbit. It is unclear which observatory (if any!) is correct, because there are no "standard candles" in the X-ray sky.

We embark on a task to establish, for the first time, such celestial standard candles and calibrate their X-ray fluxes to a 1–2% absolute accuracy. The absolute calibration will be performed by a **SmallSat**-sized mission consisting of two satellites flying in formation. A 6U-sized CubeSat will carry an absolutely calibrated X-ray source, and a companion 12U CubeSat will carry a small, simple X-ray telescope. The satellites will have separation large enough to be effectively infinite (for telescope illumination) and with precisely known distances (to predict the flux). Observations of the calibrated source, interleaved with observations of strategically chosen, non-variable celestial sources, will transfer the absolute calibration of *Cal X-1* to the celestial sources.

This will allow true end-to-end, in-orbit effective area calibrations of current and future X-ray observatories, reducing an important systematic uncertainty in the interpretation of X-ray observations. The new calibration will apply to vast archives of *Chandra*, *XMM-Newton*, *Suzaku*, *Swift*, *NuSTAR*, *NICER* and other X-ray observatories working at 1–10 keV energies, as well as future data. Thus, at a very modest cost, *Cal X-1* will significantly enhance the scientific value of billion-dollar missions.

The *Cal X-1* mission requires precision calibration of radioactive sources, precise relative navigation of two CubeSats, a miniaturized extendable boom, an efficient but vignetting-free X-ray mirror, and a CubeSat-compatible X-ray CCD camera. Each of these technologies enables *Cal X-1*, and each technology is attainable building upon existing capabilities.

2 NEED FOR ABSOLUTE X-RAY FLUXES

Many astrophysical measurements of fundamental importance rely on accurate effective area calibration of X-ray telescopes, such as *Chandra* and *XMM-Newton*. A particularly important case is cosmological constraints based on galaxy clusters. Discovering how the Universe formed and what natural forces control its evolution is one of the most basic astronomical endeavors. The cosmological model, which quantifies the various types of matter (baryonic and dark matter, massive neutrinos, dark energy) that control the geometry and expansion rate of the Universe, can be constrained in several ways. As an example, Fig. 1 shows relatively recent constraints on two interesting cosmological parameters, the Dark Energy density, Ω_Λ, and its equation of state parameter,

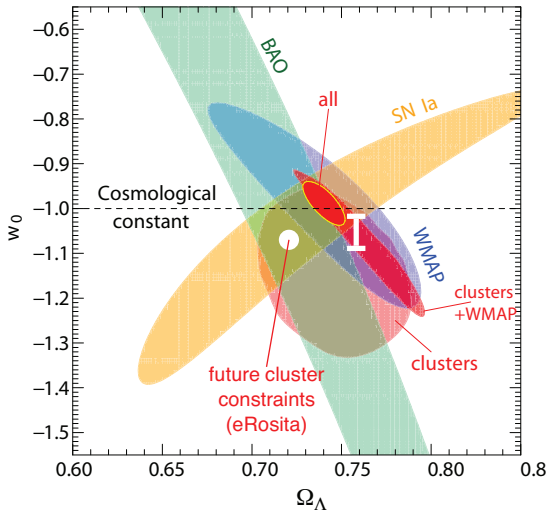

Fig. 1— Constraints on Dark Energy density and equation of state from different methods. Current cross comparisons are limited by systematic errors in absolute calibration of X-ray flux measurements. *Cal X-1* will reduce this systematic below the statistical error of the next generation of X-ray surveys.

w_0, derived from the Cosmic Microwave Background (CMB, labeled WMAP in the figure), Type 1a supernovae (SN 1a), Baryonic Acoustic Oscillations (BAO), and clusters of galaxies. The distribution of masses of clusters — the most massive gravitationally bound objects in the Universe with masses $\sim 10^{15} M_{\odot}$— is very sensitive to the cosmological model. Clusters probe cosmology in the low-z universe, while the CMB traces the state of the Universe at its dawn (z = 1000). The 'clusters' constraints in Fig. 1 are derived from *Chandra* X-ray mass measurements (Vihklinin et al. 2009) and are complementary to other methods. Combinations of all the different methods could provide the most stringent constraints (labeled 'all') if all measures agree — or indicate the need for new physics if disagreements persist. Indeed, the most recent studies hint at tension between cluster and CMB constraints, and one proposed explanation is unexpectedly massive neutrinos (Planck Collaboration 2016). It is thus vitally important to exclude the measurement errors.

Current cluster constraints are still limited by small-sample statistics, but forthcoming large X-ray emission and Sunyaev-Zeldovich (SZ) microwave background decrement cluster catalogs (e.g. eRosita, Merloni et al. 2012; SPT-3G, Benson et al. 2014) will yield order-of-magnitude tighter statistical constraints (the expected eRosita constraint is shown in Fig. 1). However, the white error bar in Fig. 1 shows the effect of a 10% systematic error on cluster masses. A bias of this magnitude will render those more accurate results systematics-limited. This problem is widely recognized by cosmologists working at different wavelengths; the Planck Collaboration (2016) noted that "Improving the precision of cluster mass calibration from the current 10% level to 1% would ... provide a stringent test of the base Λ Cold Dark Matter model." This is a recognition that "while the X-ray astronomy community has achieved extraordinary advancements in the accuracy of X-ray measurements, it seems to hit a ceiling as far as the precision of some of them is concerned" (M. Guainazzi, IACHEC, Section 12; see also **Madsen et al. Astro2020 White Paper on IACHEC**).

A cluster total mass that is used in the cosmological tests, $M_{\rm tot}$, can be determined by several methods affected by different systematics. It can be estimated most easily and reliably from the hydrostatic equilibrium method and X-ray derived gas temperature, T. Cluster temperatures currently derived by different X-ray instruments are systematically discrepant. Figure 2 shows the comparison of the temperatures from the *Chandra* ACIS and *XMM* EPIC cameras (both MOS and PN) for the same clusters (Shellenberger et al. 2015). For the hottest (and most cosmologically constraining) clusters, the difference between the *XMM* and *Chandra* derived temperatures reaches 20%. As seen from Fig. 2b, which shows the ratio of model spectra for thermal plasmas with T = 5 keV and 5.5 keV folded through the mirror and detector response, the temperature difference stems from the difference in spectral slope in the 1–10 keV band. For temperatures in this range, a 10% error in the ratio of fluxes around E = 1 keV and 5 keV would result in a 10% temperature error. Figure 2c shows the spectra of *XMM* and *NuSTAR* detectors for simultaneous observations of 3C273 (Madsen et al. 2017). Indeed, there are 10–20% energy-dependent differences between the instruments; differences with *Chandra* are of similar magnitude. These discrepancies are due to errors in the energy-dependent system efficiencies of at least one (or, more likely, all) of the large observatories. These discrepancies limit the cosmological studies using X-ray derived galaxy cluster masses. Qualitatively, $M_{\rm tot} \propto T$, so a 10% error in T results in a 10% mass error.

Other fundamental measurements, which span the range of observational X-ray astronomy from black holes and neutron stars to clusters of galaxies and the cosmic X-ray background, also rely on absolute X-ray flux calibration. We mention some of them briefly.

The classic geometric Hubble constant test derives distances to clusters of galaxies by comparing their X-ray temperatures and

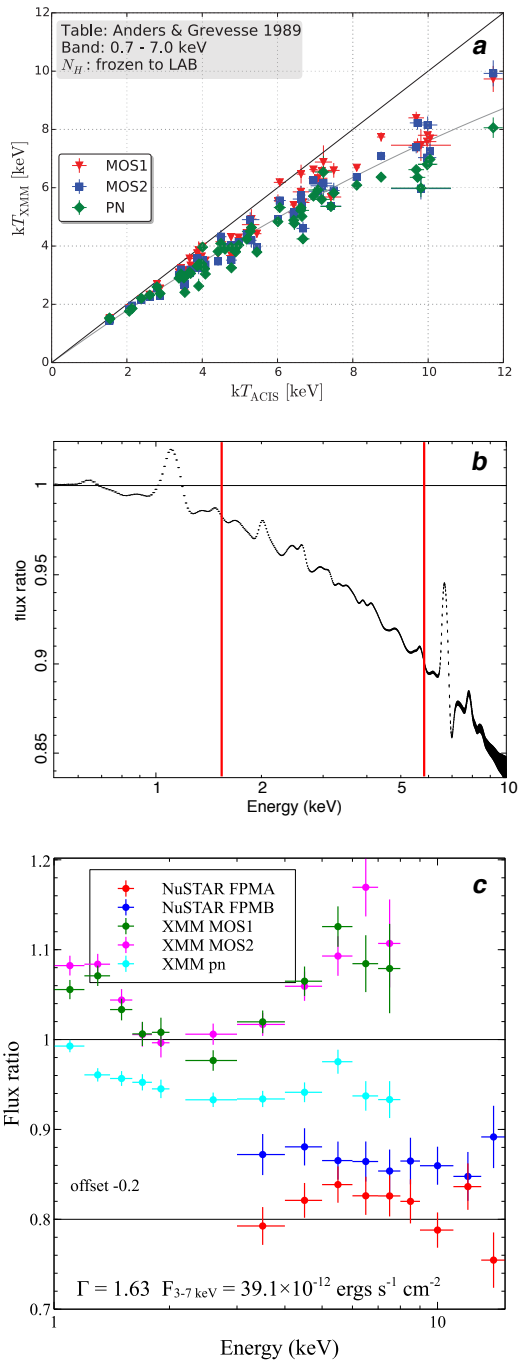

Fig. 2— (a) Cluster temperatures from *Chandra* and XMM (Shellenberger et al. 2015) show significant discrepancies. (b) The ratio of model spectra for T=5.0 keV and 5.5 keV. A 10% difference in temperature corresponds to $\sim$ 10% different ratio of fluxes around 1 keV and 5 keV. (c) The ratio of spectra of 3C273 to a common model for *XMM* and *NuSTAR* instruments (Madsen et al. 2017). There are large differences in derived fluxes for the same source observed at the same time.

fluxes to SZ microwave decrements (Silk & White 1978). The distance to a cluster, $d_a \propto y^2/(f_X T^2)$, where y is the SZ signal and f_X is the X-ray flux. A large uncertainty in these measurements stems from the X-ray calibration for f_X and T. (The uncertainty in y is beyond our scope.) If one chooses to believe that cosmology will be solved by other methods (Fig. 1), the above distance measurement enables a measurement of the Helium abundance in clusters (Markevitch 2007). Cluster cosmological tests rely on the fundamental, if unstated, assumption that cluster He abundance is at the universal average, while certain very consequential physical processes could modify it.

Determining the equation of state of the ultra-dense matter of the neutron stars requires the neutron star's radius and mass. *NICER* will provide one measure via detailed fitting of the shape and energy dependence of the phase folded light curve; a complementary measure comes from the absolute X-ray flux of Eddington luminosity of Type I X-ray bursts. A $< 3\%$ absolute flux accuracy is required to start distinguishing between the interesting equations of state (Ozel et al. 2016).

Measurements of black hole spin are made by fitting thermal continuum spectra to the accretion disk spectra of the soft state and by fitting the shape of the relativistically broadened Fe line in the reflection spectra of the hard state. These methods rely on the strong dependence of the innermost stable radius of the accretion disk on black hole spin. For the continuum method, X-ray flux is proportional to the solid angle filled with emitting material, which depends on both inclination and inner radius. Uncertainties in the absolute X-ray flux thus contribute directly to the systematic errors in derived spin (Steiner et al. 2014).

At the other end of the observational spectrum, the intensity of the Cosmic X-ray Background may provide a measure of the history of gravitational accretion integrated over cosmic time (Boldt & Leiter 1995).

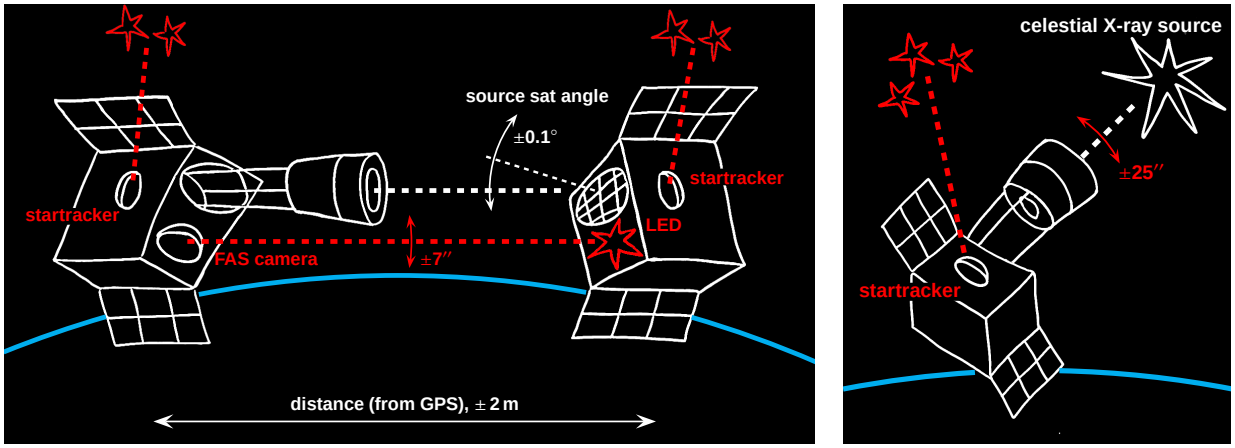

Fig. 3— *Cal X-1* (left) interleaves observations of an absolutely calibrated source with observations of the celestial X-ray standard candles. The standard candles, for example, supernova remnants G21.5–0.9 and N132D, are known to be time invariant, small in angular extent, sharply bounded, and relatively bright. The major unknown property of these standard candles is their absolute brightness, which *Cal X-1* observations will determine.

3 WHAT'S WRONG WITH GROUND CALIBRATION?

Chandra and *XMM-Newton* were both calibrated extensively prior to launch, with the goal of a $\sim 1\%$ accuracy. However, a $> 10\%$ discrepancy remains between the observatories even after attempts to reconcile the instruments over the last 15 years. Among the challenges of ground calibration is that the illumination pattern of a large-diameter X-ray mirror on the ground differs from the illumination by a celestial source at infinity. Celestial cross calibrations indicate discrepancies but cannot by themselves determine which calibration is closer to the truth. The on-board radioactive sources employed by current missions to monitor time-dependent effects in the detectors and filters cannot monitor time dependent changes to the mirror. An in-orbit, absolute, calibration standard is needed to provide both a calibration and a monitor of time-dependent system changes.

4 CAL X-1 CONCEPT

Our *Cal X-1* mission concept aims to provide two (or more) X-ray standard candles in the sky that could be used by current and future soft X-ray observatories, at a very modest cost. It will establish the standard candles at 5.9 keV, the Mn Kα line energy produced by the radioactive ^{55}Fe source, and at 1.5 keV (Al Kα line), providing calibrations above and below the atomic edge features present in all X-ray mirrors near 2 keV. In addition to providing the absolute fluxes, these are pivotal energies to pinpoint the spectral slope that determines the gas temperatures (Fig. 2b). Our goal is 2% flux accuracy at each energy, which will be a substantial leap forward from the current state of the art.

Chandra, *XMM-Newton* and other big observatories have been meticulous in calibrating the relative time dependence of their effective areas over their lifetimes by periodically observing constant celestial sources, including our primary targets. Thus a true standard candle will allow the calibration of their entire data archives. Even a *Cal X-1* measurement in $\sim$ 2023 can be applied to today's missions.

As X-ray telescopes become more powerful, the demands on calibration increase. The in-orbit effective area calibration pioneered by *Cal X-1* will be relevant to supporting large missions currently being built (*Athena*, *XRISM*) or under study (*Lynx*, *AXIS*).

5 TECHNICAL APPROACH

We propose a CubeSat mission as a low-cost (<$20M) solution to improve the calibra-

tion of Observatory-class missions (>$1B). *Cal X-1* consists of two CubeSats flying in formation, which alternately perform self-calibration operations and observations of key celestial sources.

One *Cal X-1* satellite (SrcSat) carries absolutely calibrated X-ray sources, including a bright radioactive source for 5.9 keV and a modulated X-ray source for 1.5 keV. A companion satellite (TelSat), held at a distance of 1–2 km, carries a small X-ray telescope. The telescope is alternately pointed to SrcSat and a celestial source (Fig. 3). The primary objective of *Cal X-1* is to observe two celestial sources that are already widely observed for cross calibration purposes, thus enabling the transfer of the *Cal X-1* calibration to other observatories.

The mission is **designed from the ground up to cancel out or minimize any effects of *Cal X-1* own systematics** on the celestial source calibration. For example, the X-ray mirror uses a special design that provides a large vignetting-free area around the optical axis (Fig. 5), greatly relaxing the pointing accuracy requirements.

The two satellites do not need to communicate with each other. The precision distance required for determining the absolute SrcSat flux is provided by GPS; precision pointing to the SrcSat is derived from a beacon on SrcSat and a camera on TelSat (LED beacon and FAS camera in Fig. 3). During celestial source observations, startrackers that come with the commercially procured CubeSat buses provide the required accuracy of attitude control. TelSat has a propulsion system to maintain coarse control of satellite separation.

5.1 X-ray Standard Candles

The International Astronomical Consortium for High Energy Calibration (IACHEC, Madsen et al. 2019) has identified the supernova remnants (SNR) G21.5–0.9 and N132D as good, time stationary, X-ray candles for cross calibration. While galaxy clusters are also constant, they are fainter and lack well-defined boundaries, making the finite telescope angular resolution the source of an additional uncertainty. By contrast, these SNRs are limited in angular extent, sharply bounded, and have suitable brightness for both large and small telescopes. Their *Chandra* images and spectra are shown in Fig. 4. These two SNRs have been used for in-flight effective area monitoring and cross-calibration of most major Observatories working in the 1–10 keV range. They were among the 6 verification targets observed by *Hitomi*, and will undoubtedly be used by future X-ray instruments.

We will use N132D for the 1.5 keV calibration and G21.5, which is brighter at higher energies (Fig. 4), at 5.9 keV. G21.5 provides an additional measurement at 1.5 keV, albeit with lower statistical accuracy. N132D has a radius of $\sim 1'$; G21.9 has an outer radius of $\sim 3'$, but 85% of the flux is contained in the inner core, and the remnant has an effective radius of $\sim 1'$. These sources are the subject of IACHEC spon-

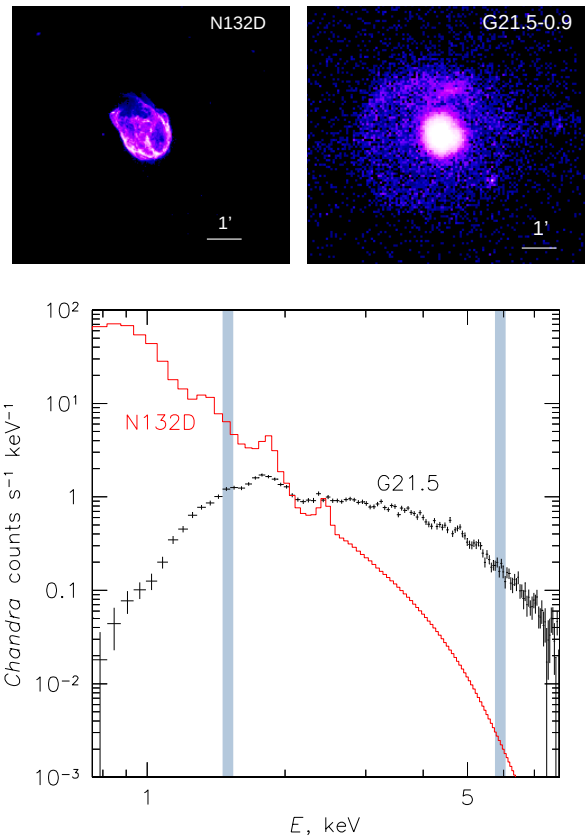

Fig. 4— *Chandra* spectra and images of the future X-ray standard candles. The *Cal X-1* calibration energies are indicated by the blue vertical bars.

sored cross-calibrations (Tsujimoto et al. 2011; Pollock & Guainazzi 2014).

Cal X-1 will observe each source for 10^6 s to achieve the required statistical accuracy. The exposures will be interleaved with SrcSat exposures. We will measure the source fluxes in narrow intervals (commensurate with the resolution of the CCD detectors of *Cal X-1* and other observatories) around the two pivotal energies. Technically, the spectral models (developed by IACHEC) will be adjusted to describe both our G21.5 and N132D observations and the SrcSat monochromatic lines, thereby **canceling out** the calibration of *Cal X-1* own instruments. G21.5 has a featureless absorbed power-law spectrum (*Hitomi* Collaboration 2018), while N132D exhibits multiple emission lines (Plucinsky et al. 2018), which will not be a concern given the well-developed model for those lines and the design of our measurement. If the mission lives longer than planned, more celestial sources can be observed.

5.2 X-ray sources

SrcSat carries precisely calibrated ^{55}Fe sources (producing the 5.9 keV Mn Kα line) and a Modulated X-ray Source (MXS) (Gendreau et al. 2012) with lines at 5.9 keV and 1.5 keV, generated by an anode constructed of Mn and Al. It is possible to use Al fluorescence (1.5 keV) induced directly by ^{55}Fe illumination, but the resulting 1.5 keV flux would be too low, hence our choice of MXS, which can provide a much brighter 1.5 keV line.

To provide the required line brightness for TelSat, the ^{55}Fe sources will have the total activity of 0.16 Ci, consisting of an array of 12 standard industrial sources in vacuum-qualified steel capsules with a Be window. The absolute intensity of each of these sources will be calibrated on the ground at National Institute of Standards and Technology (NIST) using their radioactive standard. NIST routinely calibrates radionuclidic sources to uncertainties on the order of 1%. Thereafter, the time dependence of the source flux is a simple exponential decay curve with a precisely known half-life of 2.7 yr, independent of their environment.

The ratio of the two MXS line intensities is stable and well-known — from a calibration at NIST — as a function of measurable operating conditions such as voltage and temperature. MXS will be turned on and off, while the radioactive 5.9 keV source is always on. Under the assumption of the known ratio of MXS line intensities, the intensity of the 1.5 keV line is calibrated by comparing the total 5.9 keV intensities when the MXS is on (MXS + ^{55}Fe) and off (^{55}Fe only). The MXS will be built at Goddard using commercial UHV components.

The ratio of 1.5 keV to 5.9 keV lines could be affected by organic contamination build-up on the MXS exit window after its calibration. The storage of the source in a dry N_2 environment will limit such contamination to well below the *Cal X-1* requirement ($< 0.5\mu$m of organic contamination build-up, corresponding to a transmission at 1.5 keV of > 0.993).

5.3 Telescope components

Cal X-1 carries an X-ray CCD camera at the focus of a small grazing incidence mirror supported by a one-time extendable boom. The mirror is designed from the ground up to minimize the systematics of our measurement and allow for the finite source size, pointing accuracy, and boom stability by providing a large vignetting-free region ($> 99\%$ for $r < 2'$, Fig. 5). True X-ray imaging with $\sim 1'$ PSF and the $15' \times 11'$ detector field of view ensure that we minimize the uncertainty from the PSF-scattered flux and accurately evaluate the (low) detector background.

Mirror. The X-ray mirror is based on the well-established designs of *Hitomi* and *NICER* (both built at Goddard). For *Cal X-1*, we sacrifice some effective area in order to reduce vignetting. This is achieved by shortening the primary and lengthening the secondary reflectors and having larger spacing between adjacent shells. Fig. 5*a* shows the modification to the lengths and the resulting vignetting curve. A mirror of this design with 18cm diameter and 11cm height (which can be packed into a CubeSat pre-deployment) has an effective area of 54 cm^2 at 1.5 keV and 43 cm^2 at 6 keV.

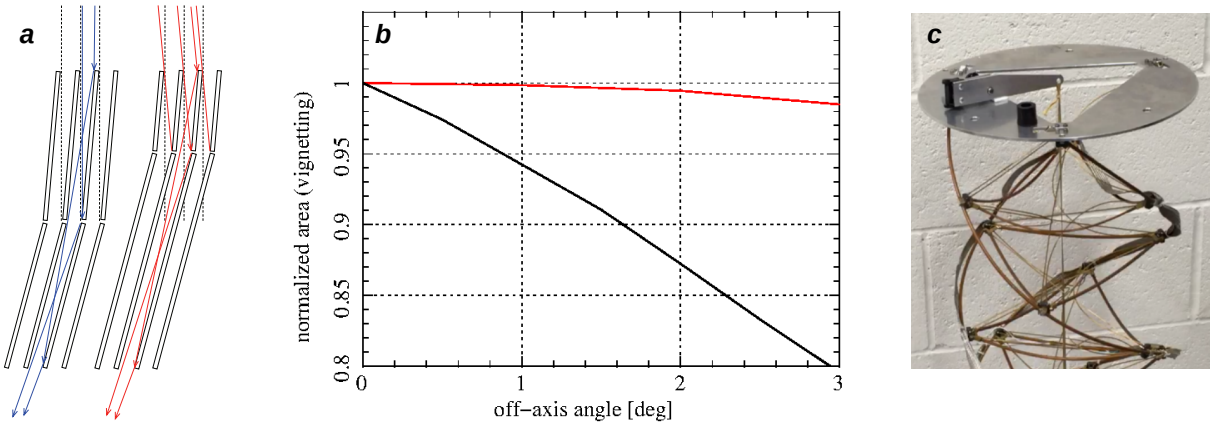

Fig. 5— The modification to primary/secondary X-ray mirror length (*a*; left is traditional design and right is modified design), which enables a vignetting-free central field of view (red curve in *b*) at the expense of some on-axis effective area. Black curve in (*b*) is for standard design. (*c*) A partially deployed coilable boom of the type that will be used to deploy the *Cal X-1* mirror, made by Orbital ATK.

Coilable boom. Orbital ATK manufactures deployable structures and coilable booms that are rigid and accurate enough to be part of astronomical telescope systems (McEachen 2011, 2013; Fig. 5c). They will supply a 2m boom that meets *Cal X-1* requirements for stability. Our concept of operations cancels out a small uncertainty of the initial placement as deployed in orbit. Pre-deployment, the boom is packed down to 2cm in height inside the CubeSat.

Detector. CCD is the workhorse of X-ray astronomy, providing a good compromise between spatial and spectral resolution. XCAM Ltd. has developed and flown optical imaging detectors on two successful CubeSats (Harris et al. 2011; AlSat 2016), and have experience with X-ray CCD camera systems for other missions. One of those CubeSats also contained a thermoelectric cooler to maintain the CCD temperature as part of the same experiment. For *Cal X-1*, we will use XCAM's off-the-shelf 385×288 pixel CCD, which will provide a $15' \times 11'$ field of view.

A proton shield and collimator with a small aperture will protect the CCD from the proton background and from stray light effects. Based on *Chandra* and *Swift* experience, we estimate the CCD background to be much lower than the source brightness at both energies, with small contributions to the error budget, even with a conservatively high estimate of a possible background Al fluorescent line (Table 1).

Cal X-1 is relatively insensitive to CCD efficiency or even contamination build up on the CCD. Both are canceled out by the observations which alternate between the calibration source and celestial source.

5.4 Relative Navigation System

The relative navigation system, employed when TelSat is pointed at SrcSat, is not yet available from the commercial CubeSat community, so it will be built at Goddard. It consists of a beacon on SrcSat, a sensor on TelSat, and an interface to the spacecraft attitude control system (ACS). SrcSat will have an array of LEDs which is unresolved at 1 km. The brightness is the equivalent of a magnitude 3 star at a distance of 2 km. The beacon will be pulsed at 1 Hz with a duty cycle of <10%. The small duty cycle allows X-ray data collection when the beacon is off, eliminating the possibility of optical background from the beacon itself.

TelSat contains a Fine Alignment Sensor (FAS) co-aligned with the X-ray telescope. To exclude parallax, the distance between the X-ray telescope and FAS is the same as that between the X-ray source and the LEDs on SrcSat. The sensor has a field of view of 9° and

the ability to centroid the LED beacon signal to $< 7''$. At the SmallSat scale, FAS is similar to the navigation system flown on the Swedish PRISMA mission. At the CubeSat scale, the FAS is similar to the optical alignment system on CANYVAL-X (Park et al. 2016).

In operation, SrcSat will point the X-ray sources and beacon anti-parallel with the direction of motion. Accuracy of better than 1° is required and easily obtained. TelSat will acquire the beacon signal and shift to an ACS control mode, which points TelSat towards SrcSat.

The *Cal X-1* error budget that includes all systematics (many of which are not discussed in this paper) is shown in Table 1. We will be able to achieve the goal of 2% flux accuracy.

6 MISSION DESIGN

A detailed design study was performed at NASA Wallops Mission Planning Lab (MPL), which specializes on CubeSats. It showed that all mechanical, thermal, power, data rate, communication, and navigation requirements can be met using mostly off-the-shelf components commercially available for the CubeSat community. The layout of the two satellites is shown in Fig. 6. The two satellite buses, 12U and 6U CubeSats, that include the ACS reaction wheels and startrackers, are offered off-the-shelf by Blue Canyon Technology. The satellites will charge their batteries during daytime and observe at night, which provides substantial power margin. The CCD will be maintained at –40°C using a thermoelectric cooler.

TelSat will have a compressed gas micropropulsion system. The orbit is selected so that, given the two satellites' ballistic coefficients, a separation of 1–2 km can be maintained with 1 propulsion maneuver per week.

The *Cal X-1* orbital requirements are given in Table 2. The altitude is driven primarily by the formation requirements and the orbit decay. The inclination is driven by the S-band communication and the desire to use NASA Near-Earth Network. The length of the mission comes from the need to observe the two celestial sources for 1 Ms each to achieve accuracies shown in Table 1. To estimate mission du-

Table 1. *Cal X-1* error budget

	Flux uncertainty[1]	
	1.5 keV	6 keV
SCIENCE REQUIREMENT		
Delivered accuracy of celestial source flux	2.0%	2.0%
EXPECTED ERROR BUDGET (L = 1 KM)		
Systematic uncertainties:[1]		
Calibration source:		
Distance L (from GPS) ..2m	0.4%	0.4%
Absolute source calibration .	1.5%	1.0%
Source sat orientation ..0.1°	0.1%	0.1%
Vignetting (off-axis angle):		
Source radius[2] .....10″		
Mirror radius[2] .....20″		
FAS pointing accuracy 7″		
Boom tilt stability ... 13″		
Total angle uncertainty 30″	0.4%	0.4%
Background uncertainty	0.5%	0.1%
Contamination uncertainty .	0.7%	0
Total cal. source systematic	1.8%	1.2%
Celestial source:		
Vignetting contributions:		
ACS pointing accuracy 25″		
Boom tilt stability ... 13″		
Source radius[3,2] ..... 60″		
Total angle uncertainty 70″	0.5%	0.5%
Background uncertainty	0.3%	0.2%
Total cel. source systematic	0.6%	0.55%
Statistical uncertainties:[1]		
Calibration source[4], 1 Ms ..	0.3%	0.3%
Celestial sources, 1 Ms each	0.25%	0.8%
Systematic + statistical:[1]		
Calibration source	1.8%	1.2%
Celestial source.....	0.7%	1.0%
Delivered accuracy (celestial + calibration sources)	1.9%	1.6%

[1] Uncertainties are 1σ. [2] Conservatively using full size as 1σ. [3] Full radius for N132D; effective radius for G21.5 at 6 keV, accounting for bright core and faint ring. [4] Assuming 0.16 Ci at time of measurement.

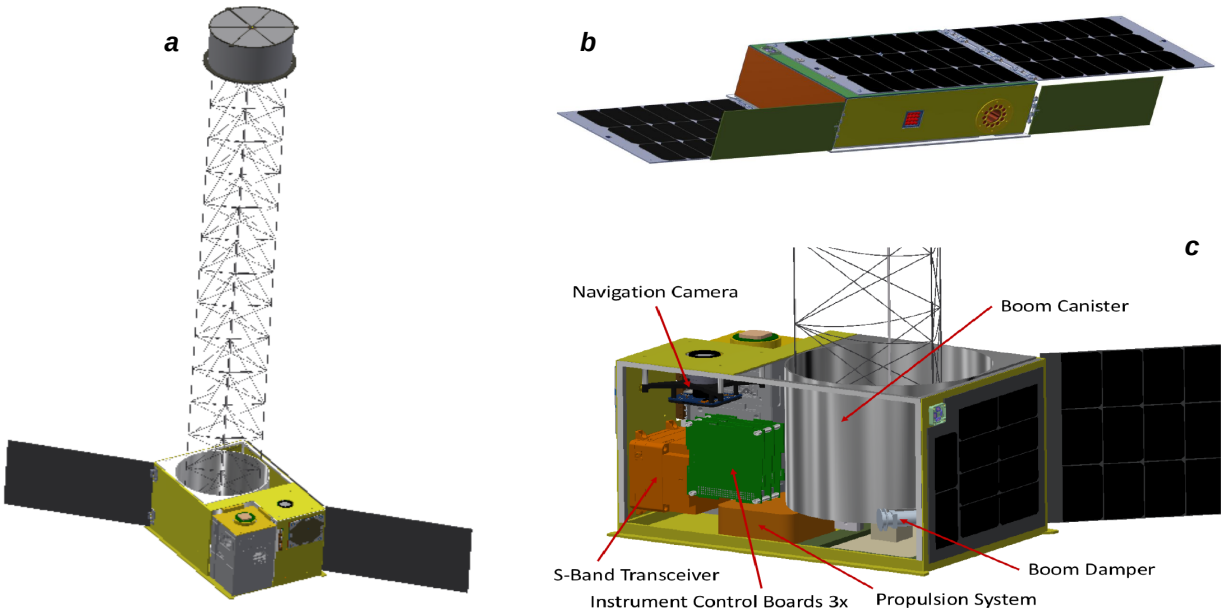

Fig. 6— *Cal X-1* mission design by NASA Wallops satellite lab. (*a*,*c*) TelSat carries an X-ray mirror on a deployable boom, CCD detector, FAS sensor, an S-band patch antenna, and a micro-propulsion unit, in a 12U CubeSat bus from Blue Canon. (*b*) SrcSat includes radioactive sources, the modulated X-ray source, and a cluster of LEDs for fine alignment with the telescope, all on the same spacecraft face of a 6U CubeSat. Both satellites have deployable solar panels.

ration, we divide 2×10^6 s by 40% (estimated fraction of night time), by 80% (estimated fraction outside SAA), by 50% (to allow observations of SrcSat) and arrive at $\sim 1.3 \times 10^7$ s, or about 5 months, which drives the primary mission length. A 6-month mission extension allows internal checks or additional targets.

The two CubeSats will be deployed together and achieve the needed separation using the TelSat propulsion system.

7 ORGANIZATION AND PARTNERSHIPS

NASA Goddard will build most of the payload that is not off-the-shelf. NIST leads absolute calibration of the radioactive sources and MXS. Collaborators from Open University (UK) lead the CCD effort. We have X-ray calibration experts from Harvard-Smithsonian CfA. The CubeSat bus will be procured from Blue Canyon Co., and we will collaborate with them on integrating Goddard's camera with their navigation algorithms. The extendable boom requires collaboration with Orbital ATK Co. All these collaborations are currently ongoing.

8 TECHNOLOGY DRIVERS

The constancy of the 1.5 keV to 5.9 keV line ratio for the MXS remains to be demonstrated. It is the subject of an ongoing internally-funded study at Goddard. The absolute calibration of the 1.5 keV line produced by MXS to the required accuracy is under current study at NIST; the current accuracy for 1.5 keV is lower than that for ^{55}Fe, which is taken into account in our estimates.

9 SCHEDULE AND COST

We have performed a mission study in 2018 for an APRA CubeSat opportunity at NASA Wallops Mission Planning Lab (MPL). The schedule, based on in-house experience, allocates 3 years from start of funding to build the components and integrate the two satellites, about 3/4 year waiting for the ride, and 1 year in orbit.

The MPL study also produced a cost estimate based on the master equipment list, ven-

Table 2. Mission Parameters

Mass (kg)	Cube size (U)	Desired orbit	Acceptable	ISS orbit OK?	In-orbit life
24 + 12	12 + 6	Altitude (km): 500	500–600	No	1 yr
		Inclination (deg): 28	28-55		

dor quotes, in-house experience for X-ray mirror manufacturing and development of navigation components (FAS), and consultations with NIST. The cumulative cost over the 5-year mission cycle (including 1 year in orbit) is $12M, of which equipment is $5M, labor $5M, and the CubeSat launch $1M. Implementing *Cal X-1* as a SmallSat (rather than APRA) will allow us to use higher-reliability bus and components, which is what we are envisioning. It will require budget reserves, and the launch will be more expensive. The total will increase but certainly stay under the SmallSat cap of $35M.

10 REFERENCES

AlSat 2016, http://space.skyrocket.de/doc_sdat/alsat-nano.htm

Benson, B., et al. 2014, "SPT-3G: a next-generation cosmic microwave background polarization experiment on the South Pole telescope", Proc. SPIE, 9153, 91531P

Boldt, E. and Leiter, D., 1995, "The Cosmic X-ray Background as a measure of history", Nucl. Phys. B, 38, 440

Gendreau, K. C. et al., 2012, "The x-ray advanced concepts testbed (XACT) sounding rocket payload", Proc. SPIE, 8443

Harris, R. D. et al. 2011, "Compact CMOS Camera Demonstrator (C3D) for Ukube-1", Proc. SPIE, 8146

Hitomi Collaboration, 2018, PASJ in press, arXiv:1802.05068

Madsen, K., et al. 2017, "IACHEC Cross-calibration of *Chandra*, *NuSTAR*, *Swift*, *Suzaku*, *XMM-Newton* with 3C 273 and PKS 2155-304", AJ, 153, 2

Madsen, K., et al. 2019, "IACHEC", Project White Paper for the Astro-2020 Decadal Survey

Markevitch, M. 2007, "Helium abundance in galaxy clusters an Sunyaev-Zeldovich effect", arXiv:0705.3289

Matheson, H. and Safi-Harb, S. 2005, "The Plerionic Supernova Remnant G21.5-0.9: In and Out", Adv. Sp. Res., 35, 1099.

McEachen, M. E., "Development of the GEMS Telescope Optical Boom". 52nd AIAA/ASME/AHS/ASC Structures, Structural Dynamics and Materials Conference, 4-7 April 2011, Denver, CO

McEachen, M. E., "Verification & Placement Precision and stability for the GEMS Telescope Optical Boom", 54th AIAA/ASME/AHS/ASC Structures, Structural Dynamics and Materials Conference, 11-18 April 2013, Boston, MA

Merloni, A., et al. 2012, "eROSITA Science Book: Mapping the Structure of the Energetic Universe", arXiv:1209.3114

Ozel, F., et al. 2016, "The Dense Matter Equation of State from Neutron Star Radius and Mass Measurements", ApJ, 820, 28

Park, J-P et al. 2016, "Mission Analysis and CubeSat Design for CANYVAL-X mission," AIAA Space Ops Conference 2016, Daejeon, Korea

Planck Collaboration, 2016, "Planck 2015 results XXIV. Cosmology from Sunyaev-Zeldovich cluster counts", A&A 594, A24

Plucinsky, P. et al. 2018, in preparation, http://web.mit.edu/iachec/meetings/2017/presentations/IACHEC2017_Plucinsky_Thermal_SNRs.pdf

Pollock, A., and Guainazzi, M., 2014, "Stability of the XMM-Newton EPIC-pn and Variability of X-ray Sources", in The X-ray Universe 2014, 302

Razdolescu, A. C. et al., 2008, "Measurement of ^{55}Fe solution activity by LSC-TDCR method", Applied Radiation and Isotopes, 66, 750.

Schellenberger, G. et al., 2015, "XMM-Newton and Chandra cross-calibration using HIFLUGCS galaxy clusters", A&A, 575, A30

Silk, J., & White, S.D.M. 1978, "The determination of qo using X-ray and microwave observations of galaxy clusters", ApJ, 226, L103

Steiner, J.F. et al., 2014, "The Low-Spin Black Hole in LMC X-3", ApJ, 793, 29.

Tsujimoto, M., Guainazzi, M., Plucinsky, P. P., et al. 2011, "Cross-calibration of the X-ray instruments onboard the *Chandra*, INTEGRAL, RXTE, Suzaku, Swift, and XMM-Newton observatories using G21.5-0.9", A&A, 525, A25.

Vikhlinin, A., et al., 2009, "*Chandra* Cluster Cosmology Project III: Cosmological Parameter Constraints", ApJ, 692, 1060.